# Noninvasive single-bunch matching and emittance monitor

A. Jansson*
*CERN, CH-1211 Geneva 23, Switzerland*
(Received 22 February 2002; published 31 July 2002)

On-line monitoring of beam quality for high brightness beams is possible only by using noninvasive instruments. For matching measurements, very few such instruments are available. One candidate is a quadrupole pickup. Therefore, a new type of quadrupole pickup has been developed for the 26 GeV Proton Synchrotron at CERN, and a measurement system consisting of two such pickups is now installed in this accelerator. Using the information from these pickups, it is possible to determine both injection matching and emittance in the horizontal and vertical planes, for each bunch separately. This paper presents the measurement method and some of the results from the first year of use, as well as comparisons with other measurement methods.

DOI: 10.1103/PhysRevSTAB.5.072803 PACS numbers: 41.85.Qg, 41.75.–i, 29.20.Lq, 29.27.Fh

## I. INTRODUCTION AND BACKGROUND

A quadrupole pickup is a noninvasive device that measures the quadrupole moment

$$\kappa = \sigma_x^2 - \sigma_y^2 + \bar{x}^2 - \bar{y}^2 \quad (1)$$

of the transverse beam distribution. Here, $\sigma_x$ and $\sigma_y$ are the rms beam dimensions in the horizontal and vertical directions, while $\bar{x}$ and $\bar{y}$ denote the beam position.

The practical use of quadrupole pickups was pioneered at SLAC [1], where six such pickups, distributed along the linac, were used. The emittance and Twiss parameters of a passing bunch were obtained from the pickup measurements by solving a matrix equation, derived from the known transfer matrices between pickups.

In rings, the use of quadrupole pickups has largely focused on the frequency content of the raw signal. Beamwidth oscillations produce sidebands to the revolution frequency harmonics in the quadrupole signal, at a distance of twice the betatron frequency, and this can be used to detect injection mismatch. This was done at the CERN Antiproton Accumulator, where the phase and amplitude of the detected sidebands were also used to find a proper correction, using an empirical response matrix [2]. However, this measurement was complicated by the fact that the same sidebands can be produced by position oscillations, which demanded that position oscillations were kept very small.

In this paper, the idea behind the SLAC method is applied and further developed for use in rings. The quadrupole pickups used for the measurements presented here were specially developed for the CERN Proton Synchrotron (PS) and optimized to measure the quadrupole moment [3]. They consist of four induction loops oriented to be sensitive to the magnetic flux in the radial direction (see Fig. 1). Since the field from a centered round beam has a flux only in the azimuthal direction, only deviations from roundness or position induce a signal in the loops. Therefore each loop is directly sensitive to the quadrupole moment, unlike previous instruments where the quadrupole moment was extracted by detecting tiny differences between four large electrode signals.

Two pickups have been installed in consecutive straight sections of the machine [4]. The optical parameters at their locations are given in Table I. As shown later, it is crucial that the pickups be installed at locations with different ratios between horizontal and vertical beta values. The phase advance between pickups is also an important input parameter in the data analysis. In order to minimize the dependence of this phase advance on the programmed machine tunes and the beam intensity (space charge detuning), the pickups were installed as close as possible to each other.

The PS pickups provide both beam position and quadrupole moment information, with bunch-by-bunch resolution, over several hundred turns. Since the beam position is also measured, its contribution to the quadrupole moment can be subtracted, leaving only the beam-size related part, $\sigma_x^2 - \sigma_y^2$. Throughout the rest of this paper, when referring to $\kappa$, it will be assumed that this "artificial centering" has been performed, unless stated otherwise.

An example of a position-corrected measurement is shown in Fig. 2, where the usefulness of the correction

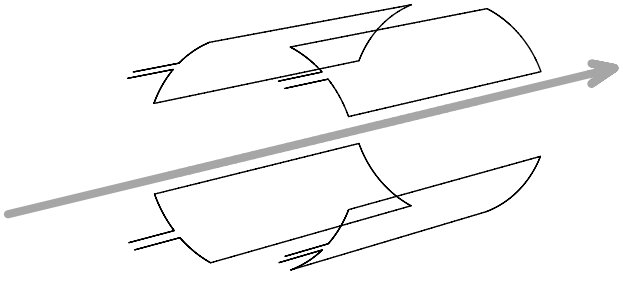

FIG. 1. Location of the induction loops. The arrow symbolizes the beam. For a centered, round beam no flux passes thru the loop and no signal is induced. Therefore, the quadrupole signal due to beam ellipticity is easy to detect.

*Email address: Andreas.Jansson@cern.ch

  

TABLE I. Beta function values and horizontal dispersion at the pickup locations. The horizontal and vertical phase advances between the two locations are also given. The pickups are installed in consecutive straight sections of the PS machine.

| Name | $\beta_x$ | $\beta_y$ | $D_x$ | $\Delta\mu_x$ | $\Delta\mu_y$ |
|---|---|---|---|---|---|
| QPU 03 | 22.0 m | 12.5 m | 3.04 m | | |
| | | | | 0.365 | 0.368 |
| QPU 04 | 12.6 m | 21.9 m | 2.30 m | | |

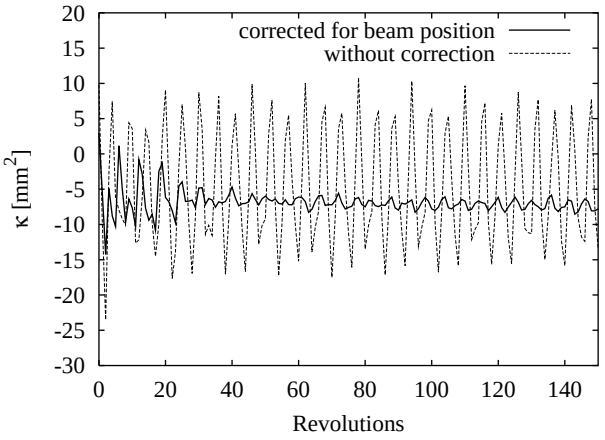


FIG. 2. Quadrupole moment $\kappa$ measured with a PS pickup immediately after injection, with and without correction for beam position. The initial beam-size oscillation is clearly visible in the corrected signal. Note the fast decoherence of beam-size oscillations, due to direct space charge.

is clear. The initial beam-size oscillation due to injection mismatch is clearly visible in the corrected signal. Note that beam-size oscillations are sensitive to the direct space charge, which means that they have a larger tune spread and therefore decohere much faster than beam position oscillations. The difference in decoherence time between beam size and position oscillations is therefore a rather direct measure of the incoherent space charge tune shift.

The detuning of the quadrupole signal frequencies can also be used to measure the incoherent tune shift, as has been done in the low energy antiproton ring at CERN [5].

## II. SIGNAL ACQUISITION AND TREATMENT

At the input to the data acquisition system, located in a building next to the machine, the analog signals from the pickup have the form

$$\Xi(t) = Z_\Xi \kappa(t - t_\Xi) i(t - t_\Xi) \quad \text{quad. moment,} \tag{2}$$

$$\Delta_x(t) = Z_\Delta \bar{x}(t - t_{\Delta_x}) i(t - t_{\Delta_x}) \quad \text{hor. position,} \tag{3}$$

$$\Delta_y(t) = Z_\Delta \bar{y}(t - t_{\Delta_y}) i(t - t_{\Delta_y}) \quad \text{ver. position,} \tag{4}$$

where the $Z$'s are the transfer impedances, $\kappa$, $\bar{x}$, and $\bar{y}$ are defined as before, and $i$ is the beam current. In the PS, the beam current is not measured by the pickup itself, so a separate beam current reference signal

$$\Sigma(t) = Z_\Sigma i(t - t_\Sigma) \quad \text{sum signal} \tag{5}$$

is taken from a nearby wall current monitor. These analog signals are sampled by digital oscilloscopes. The digitized signals are then resampled[1] to correct for the signal timing differences $t_\Xi$, $t_{\Delta_x}$, $t_{\Delta_x}$, and $t_\Sigma$. These are mainly due to cable length differences and have been measured both with a synthetic signal and by using the beam.

The analysis of the data is made in a LabView program. In order to resolve single bunches, the data are treated in the time domain, considering each bunch passage separately. The first step in the analysis is to rid the signal of its intensity dependence, by normalizing to the measured beam current. The analysis is performed in two different ways, depending on whether the position and quadrupole moment are expected to be constant or varying along the bunch.

### A. Position and size constant along bunch

If there is no variation in position and size along the bunch, and one assumes that the quadrupole pickup and the wall current monitor have the same frequency response, then the shape of a given pulse must be exactly the same in all signals (apart from a baseline offset and noise effects). The normalization problem then consists of determining the scaling factor between a pulse in the beam current signal and the corresponding pulse on the pickup outputs.

To do this, time slices of about one rf period centered on the bunch are selected. Each selected slice is a vector of $N$ samples and, under the above assumption, corresponding slices are proportional to each other. The quadrupole moment can therefore be found as the least squares solution to an overdetermined matrix equation, which in the case of the quadrupole signal has the form

$$\begin{pmatrix} \Sigma_1 & 1 \\ \Sigma_2 & 1 \\ \vdots & \vdots \\ \Sigma_N & 1 \end{pmatrix} \begin{pmatrix} \kappa \\ c \end{pmatrix} = \frac{Z_\Sigma}{Z_\kappa} \begin{pmatrix} \Xi_1 \\ \Xi_2 \\ \vdots \\ \Xi_N \end{pmatrix}. \tag{6}$$

The constant $c$ depends on the baseline difference and is not used. The same calculation is performed for the position signals, and the position contribution to the quadrupole moment is then subtracted.

An attractive feature of this method, apart from noise suppression, is that the baseline is automatically, and unambiguously, corrected for. Differences in frequency response of the two instruments could be corrected by filtering the signals, if these responses are known. However, such sophisticated corrections would enhance noise and are not necessary in the PS.

[1]Eventually, the digital resampling will be replaced by analog delay lines to improve the noise performance.

### B. Position or size varying along bunch

Sometimes, there can be a variation in oscillation amplitude and phase along the bunch. At injection into the PS, there are two main causes for this.

(i) The injection kicker pulse is not perfectly flat, which causes a variation of initial position along the bunch. The result is a fast position oscillation in those parts of the bunch that did not receive the correct kick.

(ii) If the injected beam is longitudinally mismatched, the mismatched bunch will rotate in the bucket with the synchrotron frequency, causing the bunch length to oscillate. When the bunch is tilted in longitudinal phase space there is a correlation between energy and time, apparent as a variation of the mean energy along the bunch. The degree of correlation varies as the bunch rotates, and at a position with nonzero dispersion this gives rise to a slow head-tail oscillation at twice the synchrotron frequency. Both PS pickups are installed in dispersive regions and are therefore sensitive to this effect.

(iii) There can also be a variation of the beam dimensions along the bunch, as discussed toward the end of this paper.

In these cases, the basic assumption behind the algorithm described in the previous section is no longer valid. In fact, if the position varies along the bunch, any algorithm that calculates the average position and quadrupole moment of the bunch will give an erroneous result. Since

$$\langle x^2 \rangle \neq \langle x \rangle^2, \tag{7}$$

one cannot simply use the average bunch position in Eq. (1) when correcting for the position. The correction must be done point by point along the bunch. For this purpose, a second normalization algorithm is used, which first establishes and subtracts the baseline, and then calculates the position

$$x(t) = \frac{Z_\Sigma}{Z_{\Delta_x}} \frac{\Delta_x(t)}{\Sigma(t)}, \tag{8}$$

as well as the quadrupole moment in each point. After this correction, an average beam quadrupole moment can be calculated, but it is also possible to study variations of the beam size along the bunch.

## III. BEAM-BASED CALIBRATION

### A. Internal signal consistency

One can take advantage of the position dependence of the quadrupole moment to make a consistency check between the position and quadrupole moment measurement of the pickup, using data with large beam position oscillations but stable beam size. Since the beam-size oscillations damp away much faster than beam position oscillations, such data can easily be obtained at injection by an appropriate trigger delay. A plot of expected versus measured variation of the quadrupole moment with beam position is shown in Fig. 3, showing a good agreement. This test can easily be automated and is a good indicator of whether the beam position correction works well.

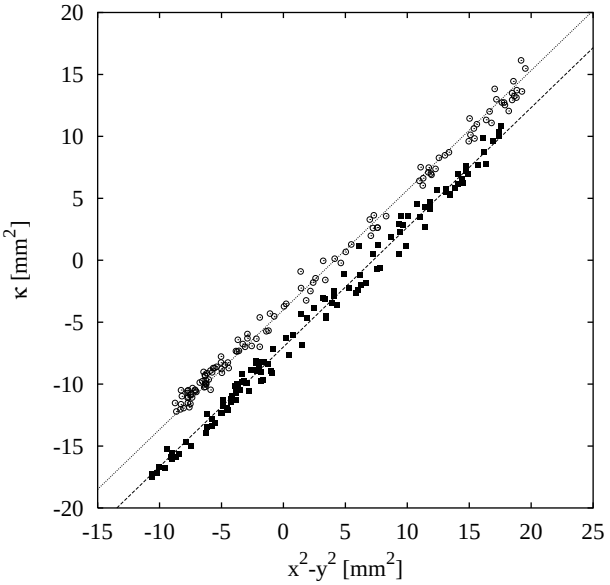


FIG. 3. Quadrupole moment (uncorrected) versus expected beam position contribution. The squares and circles represent measurements made with the same pickup on two different beams. The slope of the line is the same in both cases and is very close to 1 (0.983).

### B. Comparison with wire scanners

The standard method for emittance measurement on a circulating beam in the PS is the fast wire scanner. In order to test the calibration of the pickups, measurements were done on several different stable beams, approximately 15 ms after injection. The quadrupole pickup signal was acquired over 200 machine turns, at the same time as the wire traversed the beam. The comparative measurement was performed on all the operational beams available in the machine, with the exception of the very high intensity beams that saturate the pickup amplifiers. Thus there was a significant difference in both beam and machine parameters between the different measurements. This was done in an attempt to randomize any systematic errors. The beam parameters are given in Table II, where the different beams have been tagged with their operational names.

The rms variation in the measured quadrupole moments from turn to turn was of the order of 0.2–0.5 mm$^2$, depending on the beam intensity. Assuming that the beam size was perfectly stable, this gives an estimate of the single-turn resolution of the pickup measurement. Also the wire-scanner measurements were stable, although for some beams there was a systematic disagreement between the two wire scanners measuring in the same plane.

To compare the two instruments, the emittances measured with the wire scanners were used to calculate the expected quadrupole moment at the locations of the pickups.

TABLE II. Parameters of beams used for comparative measurements. Emittances and momentum spread are $2\sigma$ values.

| Name | $\epsilon_x$ | $\epsilon_y$ | $\sigma_p$ | $I_{\text{bunch}}$ |
|---|---|---|---|---|
| SFTPRO | 19 $\mu$m | 12 $\mu$m | $2.7 \times 10^{-3}$ | $2.7 \times 10^{12}$ |
| AD | 25 $\mu$m | 9 $\mu$m | $2.7 \times 10^{-3}$ | $3.3 \times 10^{12}$ |
| LHC | 3 $\mu$m | 2.5 $\mu$m | $2.2 \times 10^{-3}$ | $6.9 \times 10^{11}$ |
| EASTA | 8 $\mu$m | 1.4 $\mu$m | $2.5 \times 10^{-3}$ | $1.4 \times 10^{11}$ |
| EASTB | 7.5 $\mu$m | 1.4 $\mu$m | $1.6 \times 10^{-3}$ | $8.6 \times 10^{10}$ |
| EASTC | 12 $\mu$m | 3 $\mu$m | $2.4 \times 10^{-3}$ | $4.2 \times 10^{11}$ |

The momentum spread required for both the wire-scanner measurement and the subsequent calculation was obtained by a tomographic analysis of the bunch shape [6]. The propagated systematic error was estimated on the assumption that the wire-scanner accuracy is 5% in emittance, the beta function at the pickups is known to 5%, the dispersion to 10%, and the momentum spread to 3% accuracy. These estimates are rather optimistic, but give considerable propagated errors for certain measurement points. For simplicity, possible correlations between errors (e.g., beta function errors at different locations in the machine) were ignored, and all different error sources were added in quadrature. To accentuate the cases with wire-scanner disagreement, each of the four different ways of combining the two horizontal and two vertical wire scanners was calculated separately and displayed as a separate point. The result is shown in Fig. 4.

Overall, the measured data seem to indicate that the offsets are slightly smaller than measured in the lab, which could be explained by the fact that the pickups were dismantled in the lab to be moved to the machine. However, the effect is within the error bar, and no strong conclusion can therefore be made. Moreover, the pickups have been dismantled and rebuilt in the lab, without effect on the measured offsets.

The point corresponding to the EASTC beam appears to disagree somewhat in both planes, although the effect is just about within the error bar. There are a number of possible explanations for this.

(i) The PS is operated in a time-sharing mode, where a so-called supercycle containing a certain number (usually 12) of beam cycles is repeated over and over again. At the time of the measurement, the supercycle contained several instances of the EASTC beam, and it is known from experience that the position within the supercycle can affect the beam characteristics. For this particular measurement, it is not guaranteed that the measurements with the two instruments were done on the same instance of the beam, whereas for all other measurements there was either only one instance of the beam in the supercycle or the acquisition was locked to a certain instance. Some fluctuations of the measured value were also observed.

(ii) The EASTC beam has a large momentum spread and a horizontal tune close to an integer resonance. Theory indicates that the correction quadrupoles used to obtain this working point can perturb the dispersion function by more than 15% [7], which would affect both the accuracy of the wire-scanner measurement and the subsequent calculation of the expected quadrupole moment. Studies of this effect are planned for the 2002 run.

The general conclusion from the measurement series is that the wire scanner and quadrupole pickup agree within the error bar. The systematic errors due to optics parameters make it impossible to detect with certainty any difference in pickup behavior between the laboratory measurements with a simulated beam and the measurements on the real beam in the machine. In order to calibrate the

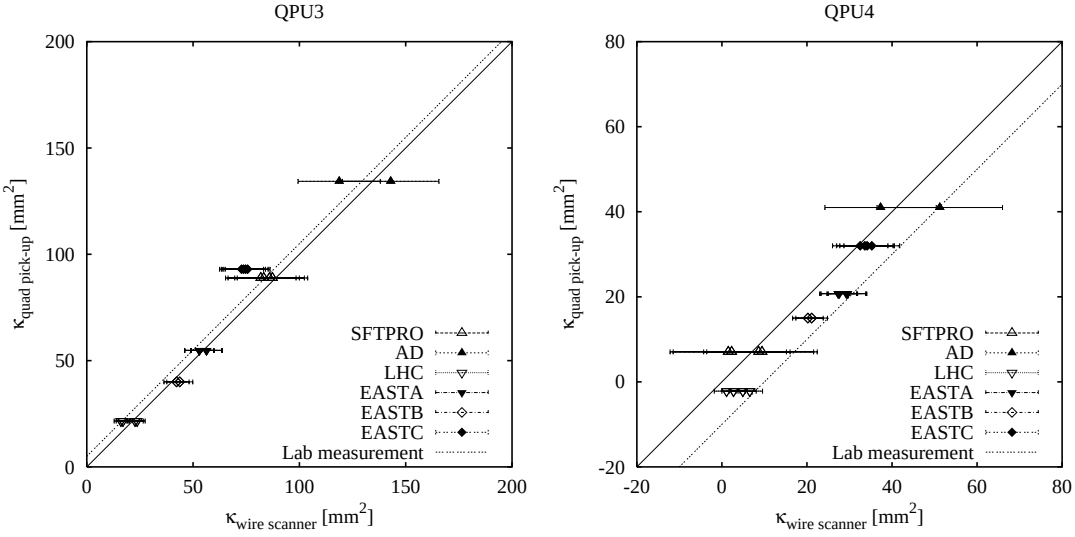


FIG. 4. Comparison between the measured value from the two quadrupole pickups and the expected results calculated from the emittances measured with the wire scanners. The solid line is the ideal case, and the dotted line includes pickup offsets measured in the lab prior to installation. All possible ways of combining the wire-scanner measurements are displayed. Note that the cases where the two wire-scanner results are inconsistent also are cases with large estimated systematic error.

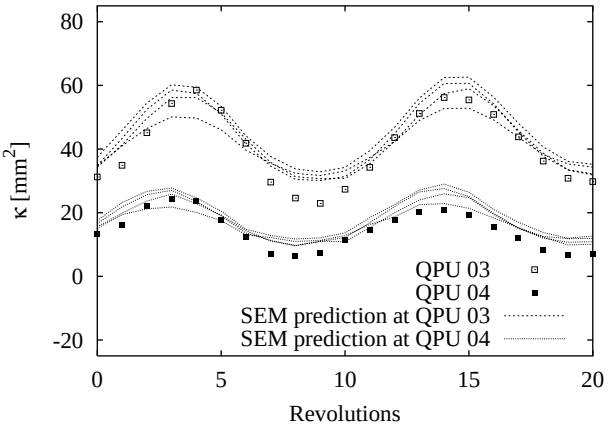


FIG. 5. Beam-size oscillations at injection measured with the quadrupole pickups and a turn-by-turn SEM grid. The SEM-grid beam-size data were used to calculate the expected quadrupole moment at the pickup locations. Beam position contributions and known pickup offsets have been subtracted from the quadrupole moments.

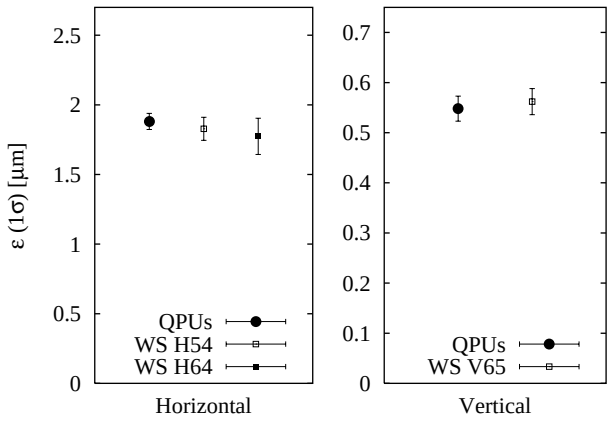


FIG. 6. Filamented emittance of a proton beam measured with quadrupole pickups (QPU) and wire scanner (WS). There is a good agreement. The error bar is the standard deviation for ten measurements. Figure from [9].

pickups accurately using the beam, the wire scanners and the pickup should be situated in the same straight section, which is excluded in the PS due to space limitations.

### C. Comparison with turn-by-turn profile measurement

Comparative measurements of injection matching have been done using a secondary emission (SEM) grid with a fast acquisition system [8] that can measure beam profiles turn by turn for a single bunch. This is a destructive device and can be used only in rare dedicated machine development sessions. It is also limited both in bandwidth and maximum beam intensity, and therefore it has not been possible to make a full systematic study on beams with different characteristics. Instead, a special beam was prepared, with low intensity to spare the grid and long bunches due to the bandwidth limitations.

The SEM-grid data were used to calculate the expected value of the quadrupole moment at the pickup locations, using the beta values, dispersion, and relative phase advance in Table I. The results are shown in Fig. 5 and show a rather good agreement with what was actually measured with the pickups. The small differences can be accounted for by systematic error sources, i.e., the optical parameters used in the comparison.

## IV. EMITTANCE MEASUREMENT

When the circulating beam is stable, the quadrupole moments of a given bunch, as measured by the two pickups, are constant and given by

$$\begin{aligned} \kappa_1 &= \epsilon_x \bar{\beta}_{x1} - \epsilon_y \bar{\beta}_{y1} + \bar{D}_{x1}^2 \sigma_p^2 , \\ \kappa_2 &= \epsilon_x \bar{\beta}_{x2} - \epsilon_y \bar{\beta}_{y2} + \bar{D}_{x2}^2 \sigma_p^2 , \end{aligned} \tag{9}$$

where $\epsilon$ denotes the emittance, $\beta$ the beta value, $D$ the dispersion, and $\sigma_p$ the relative momentum spread. The bars over certain parameters indicate that these are properties of the lattice, to be distinguished from the corresponding beam properties (typeset without the bar).

When the momentum spread is known, the system of equations can be solved for the emittances if

$$\frac{\bar{\beta}_{x1}}{\bar{\beta}_{y1}} \neq \frac{\bar{\beta}_{x2}}{\bar{\beta}_{y2}} , \tag{10}$$

which explains the earlier statement about the requirement on the beta functions at the pickup locations. If the ratio between horizontal and vertical beta functions is significantly different at the two locations, the equations are numerically stable. Thus measuring the emittance of a stable circulating beam with quadrupole pickups is in fact rather straightforward.

Statistical errors due to random fluctuations in the measurement of $\kappa$ can, although they are usually small, be reduced by averaging over many consecutive beam passages. The dominant errors are therefore systematic, coming from offsets in the pickups and errors in the beta functions, lattice dispersion, and momentum spread. The pickup offsets are, however, known from test bench measurements. Furthermore, by comparing the amplitude of position oscillations as measured by the two pickups, the ratios $\bar{\beta}_{x1}/\bar{\beta}_{x2}$ and $\bar{\beta}_{y1}/\bar{\beta}_{y2}$ can be determined.

The main uncertainty is thus the absolute value of the beta function, as for almost any other emittance measurement (e.g., wire scanner). The accuracy can therefore be expected to be comparable to that of a wire scanner. An emittance measurement using the pickup system is shown in Fig. 6, and compares well with wire-scanner results.

Note that with three pickups, suitably located, the momentum spread could also be measured.

## V. MATCHING MEASUREMENT

Even though quadrupole pickups can be used to measure filamented emittance, the main reason for installing

such instruments in the machine is to be able to measure betatron and dispersion matching at injection, as no other instrument (apart from the destructive SEM grid) is able to do this. One would like not only to detect mismatch, but also to quantify the injection error in order to be able to correct it.

### A. Matrix inversion method

To determine the parameters of the injected beam, the SLAC method [1] based on matrix inversion could be directly applied, since the quadrupole moment is measured on a single-pass basis. An advantage when performing this measurement in a ring, as compared to measuring in a linac, is that each pickup can be used several times on the same bunch. Therefore it is enough to use two pickups instead of six, which reduces both the hardware cost and the systematic error sources. It is also straightforward to improve on statistics by increasing the number of measured turns, thereby reducing noise. Another advantage in a ring is that the periodic boundary conditions reduce the number of parameters needed to calculate the matrix. Many of these parameters (tunes, phase advance between pickups, ratios between beta function values) can also be easily measured, which means that the matrix can be experimentally verified.

However, the matrix method was developed for a linac and does not take full advantage of the properties of a ring. Also, it does not include dispersion effects, and it is necessary to make assumptions on the space charge detuning when calculating the matrix.

### B. Parametric fit method

In a ring, the turn-by-turn evolution of the beam envelope, and therefore the quadrupole moment, can be expressed in a rather simple analytical formula. Expanded in terms of the optical parameters, the quadrupole moment of a beam is given by

$$\kappa = \sigma_x^2 - \sigma_y^2 = \varepsilon_x\beta_x - \varepsilon_y\beta_y + \sigma_p^2 D_x^2 - \sigma_p^2 D_y^2 , \tag{11}$$

assuming linear optics with no coupling between planes (note that there are no bars, i.e., the optical parameters here refer to the beam). If the beam is initially mismatched in terms of Twiss functions or dispersion, the value of $\kappa$ will vary with the number of revolutions $n$ performed as [10]

$$\begin{aligned}\kappa_n = {} & \bar{\beta}_x(\varepsilon_x + \Delta\varepsilon_x) - \bar{\beta}_y(\varepsilon_y + \Delta\varepsilon_y) + \bar{D}_x^2\sigma_p^2 \\ & + \bar{\beta}_x\varepsilon_x\delta_{\beta_x}\cos(2\nu_x n - \phi_{\beta_x}) + \bar{\beta}_x\sigma_p^2\delta_{D_x}^2\cos(2\nu_x n - 2\phi_{D_x}) \\ & - \bar{\beta}_y\varepsilon_y\delta_{\beta_y}\cos(2\nu_y n - \phi_{\beta_y}) - \bar{\beta}_y\sigma_p^2\delta_{D_y}^2\cos(2\nu_y n - 2\phi_{D_y}) \\ & + \sqrt{\bar{\beta}_x}\,\sigma_p^2\bar{D}_x\delta_{D_x}\cos(\nu_x n - \phi_{D_x}) .\end{aligned} \tag{12}$$

Here, $\nu_x$ and $\nu_y$ are the fractional tunes expressed in radians, and $\Delta\epsilon$ denotes the emittance increase caused by the mismatch. The first line contains constant terms and also gives the steady state value that will be reached when the oscillating components have damped away.

The two middle lines of Eq. (12) are signal components at twice the horizontal and vertical betatron frequencies. They arise from both dispersion and betatron mismatch. The betatron mismatch is parametrized by

$$\vec{\delta}_{\beta_x} = \begin{pmatrix} \frac{\beta_x}{\bar{\beta}_x} - \frac{\bar{\beta}_x\gamma_x + \bar{\gamma}_x\beta_x - 2\bar{\alpha}_x\alpha_x}{2} \\ \frac{\bar{\alpha}_x\beta_x - \alpha_x\bar{\beta}_x}{\bar{\beta}_x} \end{pmatrix} \approx \begin{pmatrix} \frac{\Delta\beta_x}{\bar{\beta}_x} \\ \bar{\alpha}_x\frac{\Delta\beta_x}{\bar{\beta}_x} - \Delta\alpha_x \end{pmatrix}, \tag{13}$$

where the last approximation is valid for small mismatch. Here, the shorthand notation $\Delta\beta = \beta - \bar{\beta}$ and $\Delta\alpha = \alpha - \bar{\alpha}$ is used for the difference between lattice and beam value.

The fourth line of Eq. (12) is a signal at the horizontal betatron frequency, which is due to dispersion matching. This mismatch is parametrized by the vector

$$\vec{\delta}_{D_x} = \begin{pmatrix} \frac{\Delta D_x}{\sqrt{\bar{\beta}_x}} \\ \frac{\bar{\beta}_x\Delta D_x' + \bar{\alpha}_x\Delta D_x}{\sqrt{\bar{\beta}_x}} \end{pmatrix}, \tag{14}$$

where, again, the shorthand notation ($\Delta D = D - \bar{D}$ and $\Delta D' = D' - \bar{D}'$) is used. There is no corresponding signal at the vertical betatron frequency due to the absence of vertical lattice dispersion. Therefore, it is not possible to distinguish vertical dispersion mismatch from vertical betatron mismatch by studying the quadrupole signal. However, one does not usually expect a large vertical dispersion mismatch.

The steady state (filamented) emittance is given by

$$\begin{aligned}\varepsilon_x + \Delta\varepsilon_x &= \varepsilon_x\frac{1}{2}(\bar{\beta}_x\gamma_x + \bar{\gamma}_x\beta_x - 2\bar{\alpha}_x\alpha_x) \\ &\quad + \sigma_p^2\frac{(\Delta D_x)^2 + (\bar{\beta}_x\Delta D_x' + \bar{\alpha}_x\Delta D_x)^2}{\bar{\beta}_x} \\ &\approx \varepsilon_x + \varepsilon_x\frac{|\vec{\delta}_{\beta_x}|^2}{2} + \sigma_p^2\frac{|\vec{\delta}_{D_x}|^2}{2} ,\end{aligned} \tag{15}$$

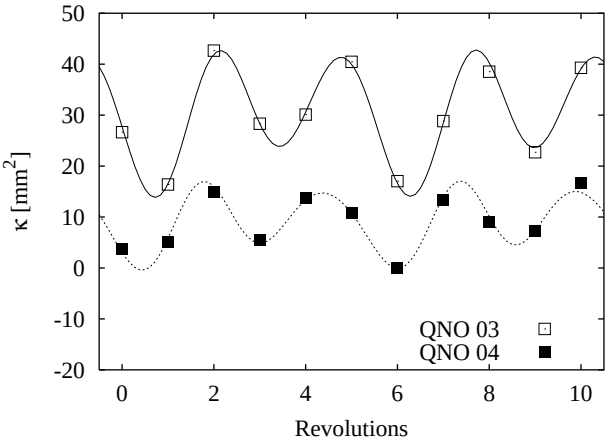


FIG. 7. Theoretical expression for the quadrupole moment fitted to measured data. Here, seven turns (14 data points) were used to determine ten free parameters (emittances, betatron and dispersion mismatches, and the tunes), but there is a relatively good match also for the subsequent turns. The measured detunings of the beamwidth oscillation frequencies were quite significant, $\Delta Q_h = 0.01$ and $\Delta Q_v = 0.05$ (as compared to the tunes measured from position oscillations).

where, again, the last approximation is valid for small betatron mismatch.[2]

By fitting the above function to the data, the injected emittances, the betatron mismatches in both planes, and the horizontal dispersion mismatch are directly obtained. The tunes can also be free parameters in the fit, which automatically estimates and corrects for space charge detuning. An example of a fit to measured data is shown in Fig. 7. A requirement for a good fit convergence is, as when measuring filamented emittance, that the ratio between beta functions should be different at the pickup locations. Also, the tunes must be such that enough independent data points are obtained. In other words, if the quadrupole signal is repetitive, it must have a period larger than the minimum number of turns required for the fit. In the PS, this means that the working point $Q_h = Q_v = 6.25$, which is close to the bare tune, should be avoided. The fit result is also less stable in the vicinity of this working point, and when the tune in only one of the planes is close to 6.25. With two pickups, at least five machine turns (ten data points) are required for the fit, if the tunes are also free parameters. Some more turns can be used to check the error, but the maximum number of turns is limited by decoherence, as discussed below.

Note that since the beam-size oscillations due to dispersion mismatch are also detuned by space charge, measuring the dispersion component separately (by changing the energy of the beam and measuring the coherent response) would result in an accumulated phase error in the dispersion term.

### C. The effect of decoherence

The fit function above does not include the effect of decoherence (damping) of the beamwidth oscillations. Fortunately, due to the physics of the decoherence process, the decay of the oscillation amplitudes is not exponential as for many other damping phenomena. If the beam is approximated by an ensemble of harmonic oscillators with a tune distribution $\rho(\Delta Q)$ and an average tune $Q$, its coherent response to an initial displacement is

$$x(s) = e^{i2\pi Qs} \underbrace{A_0 \int_{-\infty}^{\infty} e^{i2\pi \Delta Q s} \rho(\Delta Q)\, d(\Delta Q)}_{A(s)}, \qquad (16)$$

and the derivative of the amplitude function

$$\frac{\partial A}{\partial s} \propto \int_{-\infty}^{\infty} e^{i2\pi \Delta Q s} \Delta Q \rho(\Delta Q)\, d(\Delta Q) \qquad (17)$$

is zero at $s = 0$, i.e., initially the amplitude is unchanged by the decoherence process. A plot of the amplitude versus time for some tune distributions is given in Fig. 8, showing that the initial behavior is also largely independent of the distribution.

In reality, the tune of each individual particle is changing with time (e.g., due to synchrotron motion), and therefore the decoherence pattern is more complicated. However, synchrotron motion is negligible for the first few turns. Therefore, data analysis is greatly simplified and accuracy is improved, if one limits the number of turns to a rather small value. This also demonstrates an advantage of the fit method over a fast-Fourier transform (FFT) analysis of the signals, since an FFT needs many points to achieve good frequency resolution.

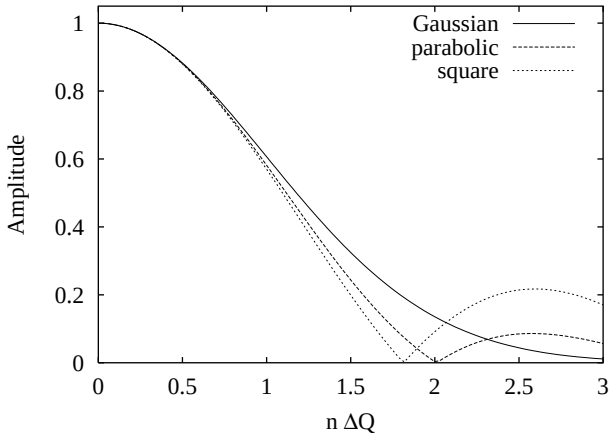


FIG. 8. Evolution of coherent amplitude during decoherence, for three different momentum (tune) distributions. Here, $\Delta Q$ is the rms tune spread and $n$ is the number of revolutions.

[2]There is also a contribution to the emittance increase due to injection miss steering that is not included here, since normally coherent dipole oscillations filament much slower than quadrupole oscillations, and the beam position contribution is subtracted from the signal.

### D. Measurement results

To test the injection matching measurement, a series of measurements was done with different settings of some focusing elements of the PS injection line. An example of such a measurement is shown in Fig. 9, where a quadrupole was changed in steps of 10 A, and the resulting variation of the fit parameters recorded. The variation of the different error vectors expected from beam optics theory is also shown, and there is a rather good agreement, both in direction and magnitude of the changes. The injected emittances are unchanged, as expected.

By using the theoretical response matrix for dispersion and betatron matching, a proper correction to the measured error can be calculated [11]. So far, actual corrections of the measured mismatches have not been made, since the dominant error (the dispersion mismatch) cannot be corrected without a complete change of optics of the entire line. Studies for a new dispersion matched optics are underway.

While the dispersion mismatch is large for all beams, due to the transfer line design, the level of betatron mismatch varies between different operational beams. Most high intensity beams measured were observed to be fairly well matched, whereas some lower intensity beams had a significant mismatch. This might be explained by the fact that mismatch is likely to cause losses for aperture limited beams, and therefore the process of intensity optimization leads to well-matched beams, although the mismatch is never directly measured. This indirect matching mechanism is absent for the future bright Large Hadron Collider (LHC) beam, and it can therefore be expected to develop a relatively large mismatch if not continuously monitored and corrected.

## VI. MEASUREMENT WITHIN THE BUNCH

As mentioned earlier, the transverse mean position can sometimes vary along the bunch. However, in some cases, also the beam size itself varies along the bunch. This is notably the case for high intensity beams that are highly non-Gaussian. For a Gaussian beam distribution, the transverse bunchwidth is constant along the bunch. This is because the multidimensional Gaussian is just a product of one-dimensional Gaussians. However, for a parabolic beam this is no longer true, as may be easily verified analytically.

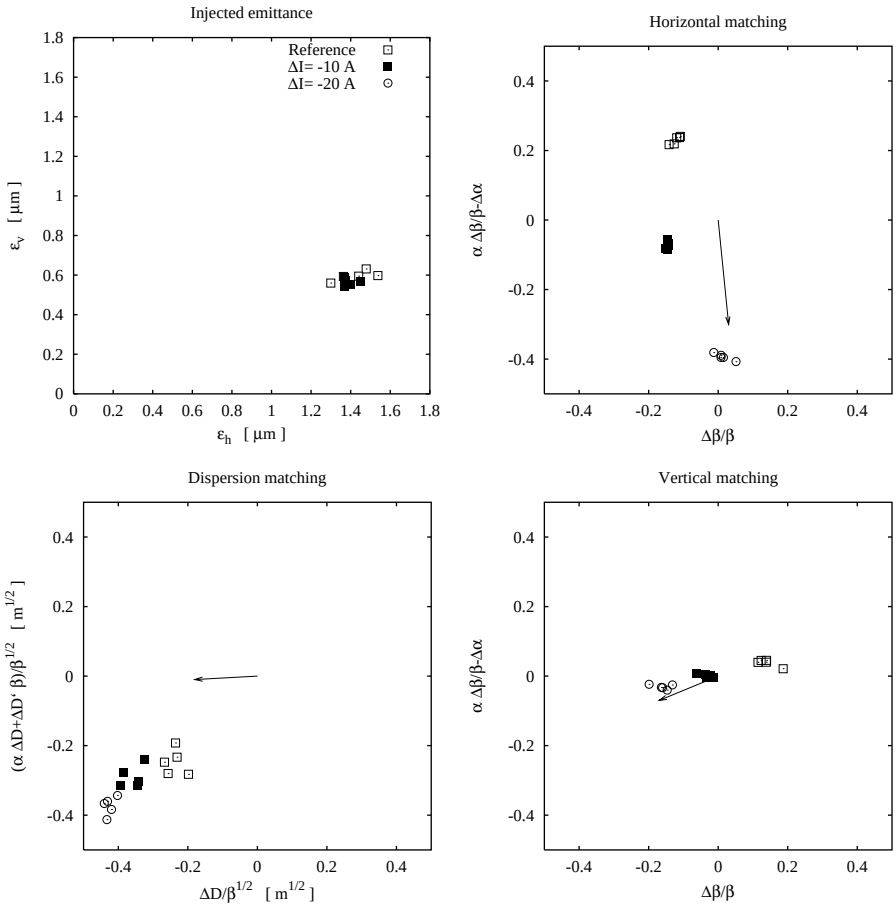


FIG. 9. Injected emittance, betatron, and dispersion mismatch vectors for three different settings of a transfer line quadrupole. Note the large dispersion mismatch. The vectors illustrate the variation in mismatch that is expected for a correction of −10 A (calculated from beam optics theory). There is a good agreement between expected and measured behavior, indicating that the measurement works well.

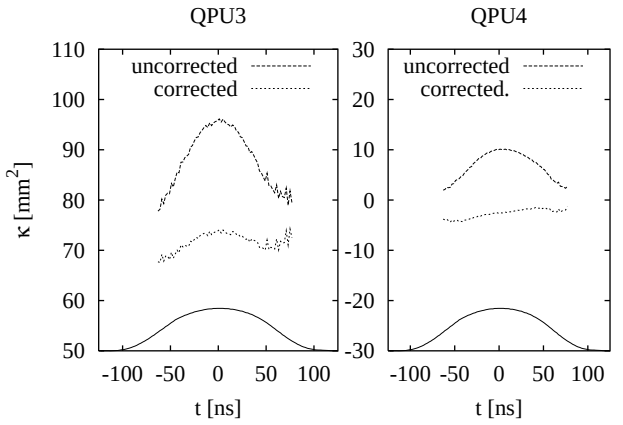


FIG. 10. Quadrupole moment as a function of position within the bunch, with and without correction for dispersive contribution. The bunch shape is also indicated (solid line).

With the pickups, it is possible to measure the quadrupole moment as a function of position within the bunch. The measurement is good over most of the bunch, but naturally gets very noisy and prone to systematic errors in the head and tail, since these regions are sparsely populated. A measurement made on a stable beam is shown in Fig. 10. The plot also shows the same measurement with the dispersion contribution subtracted,[3] indicating that the variation of beam size along the bunch is mainly due to variations in momentum spread. This fits with the fact that the longitudinal bunch distribution is usually non-Gaussian. Applying the methods discussed earlier on the dispersion corrected data, it is also possible to calculate the emittance variations along the bunch.

## VII. CONCLUSIONS

The quadrupole pickups recently built and installed in the PS machine have been evaluated in a series of measurements. These pickups measure both injection matching and emittance for a single, selected bunch in the machine. The measurement can be made parasitically, without perturbing the beam, because the devices are nonintercepting.

Comparisons with other instruments in the machine show good agreement. All observed deviations are within the estimated systematic error bars. The systematic errors come mainly from the imperfect knowledge of beta value and dispersion needed to evaluate the data. Systematic errors are indeed expected to dominate the total error in the quadrupole pickup measurement, as is the case for most emittance measurement devices.

For matching applications, the pickups can be used to determine phase and amplitude of horizontal and vertical betatron mismatch, as well as horizontal dispersion mismatch. This analysis can be done individually on each injected bunch. Since the mismatch is detected as an oscillation, the effect of systematic errors (e.g., pickup offsets) is not very important.

As emittance measurement devices, the pickups have some interesting properties. The single-turn resolution makes it possible to measure and follow the evolution of the emittance over many turns (limited only by acquisition memory). When measuring filamented emittance, it is possible to reduce the effect of noise by averaging over many turns, and also to check that the beam is stable during the measurement, something that is assumed but not actually verified during a wire-scanner measurement. More important, the pickups have no moving parts that wear out, as is the case for a wire scanner. This makes it possible to create a watchdog application to monitor the evolution of the emittances pulse by pulse over a long period. In such an application, systematic errors are again of lesser importance, since variations rather than absolute values are sought.

The pickups can also be used to study variations of the emittance along the bunch, although this may be mainly of academic interest.

## ACKNOWLEDGMENTS

The author would like to thank D. J. Williams and L. Søby for their support and important contributions to the pickup hardware, H. Koziol for reading and commenting on an early draft of this paper, and U. Raich and C. Carli for contributing to the turn-by-turn SEM-grid data acquisition and analysis.

[3] The momentum spread as a function of position within the bunch was obtained from a tomographic analysis [6] of the bunch shape data.

[1] R. H. Miller *et al.*, in *Proceedings of the 12th International Conference on High Energy Accelerators, Batavia, 1983* (Fermilab, Batavia, IL, 1983).
[2] V. Chohan *et al.*, in *Proceedings of the 2nd European Particle Accelerator Conference, Nice, France, 1990* (Editions Frontieres, Gif-sur-Yvette, France, 1990).
[3] A. Jansson and D. J. Williams, Nucl. Instrum. Methods Phys. Res., Sect. A **479**, 233 (2002).
[4] A. Jansson, L. Søby, and D. J. Williams, in *Proceedings of the 5th European Workshop on Beam Diagnostics and Instrumentation for Particle Accelerators, Grenoble, France, 2001* (ESRF, Grenoble, France, 2001).
[5] M. Chanel, in *Proceedings of the 5th European Particle Accelerator Conference, Sitges, Spain, 1996* (IOP, Bristol, U.K., 1996), pp. 1015–1017.
[6] S. Hancock *et al.*, in *Proceedings of the Conference on Computational Physics, Granada, Spain, 1998* [Comput. Phys. Commun. **118**, 61–70 (1999)].
[7] C. Carli (private communication).
[8] M. Benedikt *et al.*, in *Proceedings of the 5th European Workshop on Beam Diagnostics and Instrumentation for Particle Accelerators, Grenoble, France, 2001* (Ref. [4]).

[9] A. Jansson and L. Søby, in *Proceedings of the 19th IEEE Particle Accelerator Conference, Chicago, IL, 2001* (IEEE, Piscataway, NJ, 2001).
[10] A. Jansson, Ph.D. thesis, Stockholm University, 2001.
[11] M. Giovannozzi, A. Jansson, and M. Martini, in *Proceedings of the Workshop on Automatic Beam Steering and Shaping, Geneva, Switzerland, 1998* (published as CERN Yellow Report No. CERN 99-07).